

# Return Period for the Maximum Daily Rainfall in Eastern Highlands of Jordan Valley.

<sup>1</sup>EMAD AKAWWI \*, <sup>2</sup>METRI MDANAT

<sup>1</sup>Faculty of Engineering, Al-Balqa Applied University, Al-Salt, 19117, JORDAN;

<sup>2</sup>School of management and logistic sciences, German Jordanian University, Madaba, JORDAN

*Abstract-* Daily rainfall data for the last 30 years was used in the study area. Various available plotting position formulae were employed to evaluate different return periods. Different statistical analyses of maximum daily rainfall were undertaken. The best-fit curves were the Gumbel and Log-Pearson type III (3LP). As a result, the  $X_t$  for the Log-Pearson type III and the Gumbel plotting position, which has the lowest RMSE as the best fit values for the return periods.

Key-words: -Jordan, Mean, Rainfall, Return Level, Return Period, Standard Deviation, Statistical.

Received: June 23, 2021. Revised: March 17, 2022. Accepted: April 14, 2022. Published: May 10, 2022.

## 1. Introduction

Water scarcity occurs at the time of the demand of surface and subsurface freshwater more than the supply in any specific area due to a physician shortage in storage water, inappropriate infrastructures to a depot, distribute and access water [1]. Natural and Human processing affects practically all sections of the hydrological cycle. Human activities like to cut trees and clear the forest, afforestation, and agriculture have uncomfortable influences on the hydrological cycle, including evapotranspiration, groundwater level, surface sea level, and water flow regimes. Human activities influence cloud formation [2]. Observational studies and climate projections provide plenteous proof that water resources vulnerable and have the prospect to be powerfully wedged by global climate change, with wide-ranging outcomes for ecosystems and human beings' societies [3].

Changes in surface and groundwater resources are especially relevant in locations where water availability is an abbreviate factor for social and economic development. As one of the Mediterranean regions, the Middle East is a "hot-spot" region in terms of water shortage and climate changes. Generally, as most of the Middle East countries, Jordan depends entirely on precipitation for its renewable water resources. Most of the researchers in the water management define that 83% of Jordan has low-rainfall areas in which 90% of annual rainfall does not reach 200 mm/year. The mean annual precipitation in Jordan is estimated to be about 110 mm in 2009 2010 [4]. Haddadin et al.[5] discussed the water shortage in Jordan and the significant elements of sustainable water solutions. [6] studied the water condition in

Jordan by investigating a sample of a fifteen-year record for water use. Decreasing in rainfall will lead to a significant lack of surface runoff and groundwater recharge processes in the Zarqa River Basin [7].

Referencing climate model analyses made by [8] shows that the people at danger because of increasing water scarcity with rising temperatures. The future global climate change might influence public and water demand in the industrial sector, yet as a competitor with the need for water use for agricultural irrigation [9]. Probabilistic distributions can be used in the studies such as the management of water resources and the reporting of practical factors about the hydrologic cycle. Many researchers attempted to select the best-fit model locations and estimate the desired rainfall for different return periods. Annual maximum daily precipitation for managing water resources was used by several researchers to find the return periods of rain. Prediction of rainfall using different probability distributions for specific return periods was studied by [10]. [11] have researched about analysis of rainfall records to determine the characteristic of the observed frequency distributions. [12] found that Generalized Extreme Value, the distributions Pearson type III and Log-Pearson type III, showed the most significant number of best-fit results for the maximum monthly rainfall. The statistical methods were used by [13] estimated the missing rainfall data and compare their results with the current methods.

The main question of this research is: what is the best-fit probability distribution for the maximum daily rainfall return period of the study area? This study's objectives are to apply the statistical analysis of the rainfall for the last thirty-one years (1988-2018). The main aim is to find the best-fit probability distribution for the study area, which yields the maximum day

annual rainfall for return periods of 2, 3, 5, 10, 15, 25, 50, and 100 years by using different plotting position curves and the Probabilistic suitable distributions. These results can give useful guidance for policy and decision-making purposes.

## 2. Study Area

The study area located to the eastern part of the Jordan Valley as shown in the map (figure 1). These Governorates shows significant differences in elevations above mean sea level. Heights can go from less than zero below mean sea level to more than 1240 m.

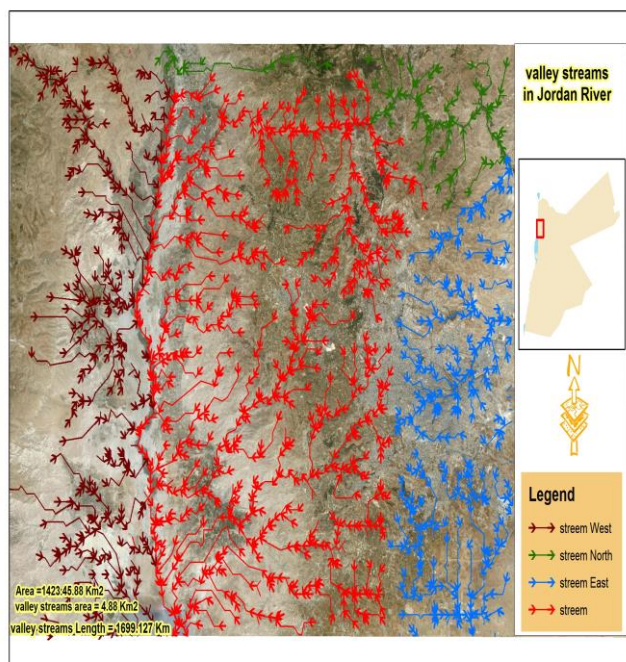


Figure 1. Shows the map of drainage of the study area (the study area represents by rectangle in Jordan Map to the right).

The study area is characterized by a hot summer (June – September). The temperature starts rising from the beginning of May and increasing to a peak in the month of august at 42°C. The winter season is starting with November and ending in March. The coldest month is January with a minimum temperature of 0 °C and may reach to -5 at night in several days.

## 3. Methods and Materials

### 3.1. Data Management

The precipitation data and the temperature collected from the meteorological department and the water and irrigation Ministry for a hydraulic cycle for

the period (between 1988 and 2018). This work was based on an extensive and comprehensive database of meteorological data (rainfall and temperature). All data were input and analyzed statistically by using Microsoft (Excel).

### 3.2. Analysis of Annual Rainfall Data

The annual rainfall data obtained from the meteorological department and irrigation and water ministry for the last 30 years (1988 – 2018) were analyzed and standardized.

The histograms and other plots were created for the rainfall data. The statistical parameters as the arithmetic mean (average), standard deviation, coefficient of variation, and co-efficient of skewness of annual rainfall were calculated by using the formulas listed in Table 1.

The annual precipitation data is analyzed over the study area regarding the statistical parameters. The best fit distribution method is determined using various plotting positions and probabilistic distribution methods, as listed in Table 1.

**Table 1.** The Statistical Parameters that were used in this study.

Name	abbreviatio n	Rules	Information
Mean (Average)	$\mu, X_{Avr}$	$\sum X_i/n$	$X_i$ : the rainfall intensity (mm), $n$ is number of the sample, $i= 1,2,\dots,n$
Standard Deviation	$\sigma$	$[\sum(X_i - \mu)^2 / (n-1)]^{1/2}$	$X$ is the rainfall amount, $n$ is the sample length, and $i=1,2,\dots,n$
Co-efficient of Variation	$C_v$	$(\sigma / \mu) \times 100\%$	$\mu$ is the mean, and $\sigma$ is standard deviation
Co-efficient of Skewness	$C_s$	$1 / \sigma^3 * [N/N^2 - 3N+2] * [\sum(X_i - \mu)^3]$	$\sigma$ is standard deviation, $N$ number of years, $\mu$ is mean, and $i=1,2,\dots,n$

Several Probabilistic distributions with its parameter estimation are used in this study, as shown in table-1, and they are explained in the following sections. The

$$\sigma_Y = \sqrt{\ln\left(1 + \frac{\sigma_x^2}{\mu_x^2}\right)} \tag{1}$$

$$\mu_Y = \ln(\mu_X) - \frac{1}{2} \sigma_Y^2 \tag{2}$$

variable X represents observed data, while x represents any possible value of that data and is used to create the distribution functions, as shown in the next sections.  $F_X(x)$  is the value of the distribution function for the point where x corresponds to  $X$ 's observed data value.

### 3.3.1. Normal Distribution

The normal distribution is applied in a maximum daily annual rainfall and runoff analysis [14]. The two moments, average ( $\mu$ ) and variance ( $\sigma^2$ ), are the main parameters of the normal distribution. The probability density function (pdf),  $f(x)$  and cumulative distribution function (cdf) and  $F(x)$  for a standard random variable x are created by using the following formulas:

$$f(x) = \frac{1}{\sigma\sqrt{2\pi}} \exp\left[-\frac{1}{2\sigma^2}(x-\mu)^2\right] \quad (3)$$

$$F(x) = \frac{1}{\sigma\sqrt{2\pi}} \int_{-\infty}^x \left(\exp\left[-\frac{1}{2\sigma^2}(x-\mu)^2\right]\right) dx \quad -\infty < x < \infty \quad (4)$$

$$F(x) = \frac{1}{\sigma\sqrt{2\pi}} \int_{-\infty}^{\infty} \left(\exp\left[-\frac{1}{2\sigma^2}(x-\mu)^2\right]\right) dx \quad -\infty < x < \infty$$

$$F(x) = \frac{1}{\sigma\sqrt{2\pi}} \int_{-\infty}^{\infty} \left(\exp\left[-\frac{1}{2\sigma^2}(x-\mu)^2\right]\right) dx \quad -\infty < x < \infty$$

### 3.3.2. Two Parameters Log-Normal Distribution (LN2)

The (pdf) and (cdf) of the 2-parameter Log-normal distribution are expressed as the following rules:

$$f(x) = \frac{1}{x\sigma_Y\sqrt{2\pi}} \exp\left[-\frac{1}{2\sigma_Y^2}(\ln(x) - \mu_Y)^2\right] \quad (5)$$

$$F(x) = \frac{1}{\sigma_Y\sqrt{2\pi}} \int_0^x \frac{1}{x} \exp\left[-\frac{1}{2\sigma_Y^2}(\ln(x) - \mu_Y)^2\right] dx \quad (6)$$

The range of the random variable is  $x > 0$ . The logarithm of the x variable,  $y = \ln(x)$ , is well-described by a normal distribution. By using the method of moment estimators, the parameters are created as the following formulas:

Are the commonly used parameters of the Log-Normal distribution. Here,  $\sigma_Y$  is the standard deviation, and  $\mu_Y$  is the mean for this distribution.

### 3.3.3. Log-Pearson Type III

Log-Pearson Type III is one of the gamma family distribution. This distribution describes a random variable X, whose logarithm follows the Pearson type III distribution. The pdf and cdf of log-Pearson type III were calculated by using the following formulas:

$$f(x) = \frac{1}{|\alpha|x\Gamma(\beta)} \left[\left(\frac{\ln(x)-\xi}{\alpha}\right)^{\beta-1} \exp\left[-\frac{\ln(x)-\xi}{\alpha}\right]\right] \quad (7)$$

$$F(x) = \frac{1}{|\alpha|\Gamma(\beta)} \int_0^x \frac{1}{x} \left[\left(\frac{\ln(x)-\xi}{\alpha}\right)^{\beta-1} \exp\left[-\frac{\ln(x)-\xi}{\alpha}\right]\right] dx \quad (8)$$

The parameters scale " $\alpha$ ," shape " $\beta$ " and location " $\xi$ " is estimated by using the method of moment estimators as the following:

$$\beta = 4/\gamma^2 \quad (9)$$

$$\alpha = \sigma\gamma/2 \quad (10)$$

$$\xi = \mu - 2\sigma/\gamma \quad (11)$$

### 3.4. Goodness-of-fit Tests

These tests are used for evaluating the validity of a specified or assumed probabilistic model. This test can be applied by using several methods as plot method, numerical method, and formal normality test. In this study, the Plot methods and the root mean square error (RMSE) was used to evaluate the best model.

#### 3.4.1. Root Mean Square Error (RMSE)

This method indicates that the smallest RMSE value is the best-fit model. It measures the difference between estimates and observed values. It can be calculated using the following formula:

$$RMSE = \sqrt{\frac{1}{n} \sum_{i=1}^n (x_i - X)^2} \quad (12)$$

$x_i$  is the observed value, and X is the estimated number.

### 3.4.2. Graphical Test

It is the most suitable test for determining the best-fit model. The Q-Q plot of observed and estimated values is used. Several plotting positions were used for specific distributions to calculate the plotting position of the non-exceedance probability, as mentioned in table 2. Most of the plotting position formula that was used here have the following formula:

$$P_{i:n} = \frac{n - a}{N + 1 - 2a} \quad (13)$$

$n$  is the rank of the observed value  $X$  ( $X(i)$  is ascending order),  $n = 1, 2, \dots, N$ .  $N$  is the total number of observations.

Gumble plotting position, which gives unbiased quintiles; Gringorten's plotting position ( $a = 0.44$ ); Cunnane's plotting position ( $a = 0.4$ ) [15]. The observed data,  $\mathbf{X(i)}$ , against the estimated values,  $\mathbf{x(F)}$  (the quantile function), are plotted to create the Q-Q plot, with  $\mathbf{F}$  identify by the  $\mathbf{p_{i:n}}$  for the specific distribution.

### 3.5. Return Period (T)

The main important target of frequency analysis is to find the return period. If the variable ( $x$ ) equal to or greater than an event of magnitude  $x_t$ , occurs once in  $T$  years, then the probability of occurrence  $P(X \geq x)$  in the given year of the  $X$  (Variable) is:

$$P(x \geq x_T) = \frac{1}{T} \quad (14)$$

$$T = \frac{1}{1 - P(x \leq x_T)} \quad (15)$$

The rainfall amounts related to the 50- or 100-year return periods cannot be directly estimated from a data set. They can be generated from the 98<sup>th</sup> and 99<sup>th</sup> percentiles for the 50 years and the 100 years return period, respectively, of a fitted distribution [16].

## 4. Results and Discussions

The methodology motioned in the previous sections was developed to the 31 years observational data in which lists the maximum daily rainfall in millimeters ( $mm$ ) was gotten from irrigation and water ministry and department of Meteorology.

The distribution of annual precipitation all over Jordan was summarized in figure-2 the study area of Ajlun governorate located within the range of yearly rainfall capacity of 700 to 900 mm/year.

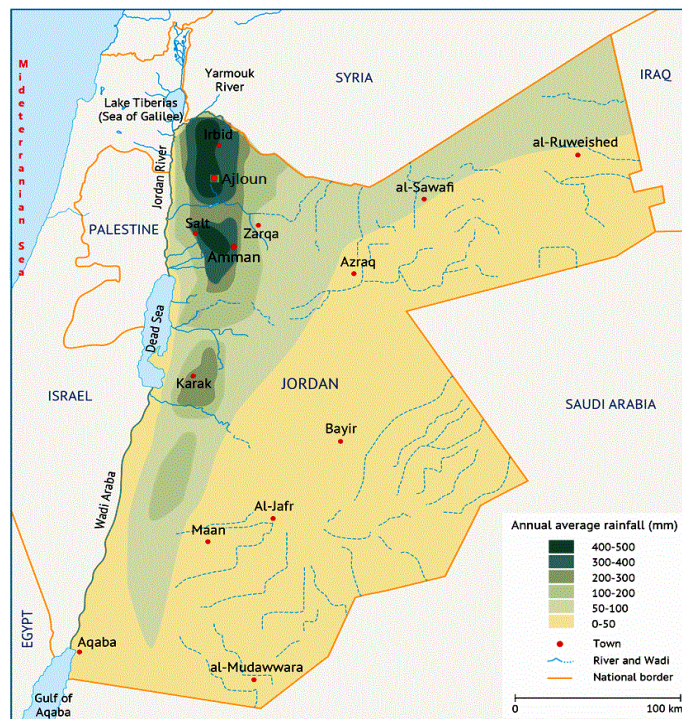


**Figure 2.** the annual precipitation all over Jordan, Ajlun and Al-Salt governorates located within the range of 700 – 900 mm/Y.

### 4.1. Statistical Analysis

The histogram of the annual rainfall distributions for the 31 years (figure-4) shows that the total precipitation in the last decade (2009-2018) for about 4949 mm, while the total rainfall for the decade (1999 – 2008) was 4809 mm and for a decade (1989 – 1998) was about 5849 mm. This information for the total rainfall shows that the total rainfall in the decade (1999 – 2008) and decade (2009 – 2018) decreased by about 17% compared to the decade (1989-1998). On the other hand, the total rainfall is almost the same for the decades (1999 – 2008) and (2009 – 2018). The maximum daily rain was between 26 mm and 131 mm.

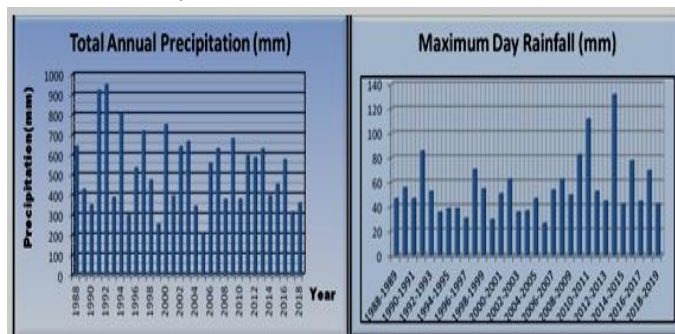


**Figure 3.** Annual rainfall (Lift) and the Maximum Day Annual Rainfall (Right) distributed for the period of 31 years (1988-2018).

The results of the statistical parameters are calculated and listed in table- 2.

**Table 2.** Plotting Position Methods and Probabilistic Distribution Methods.

Plotting Position Method	Value of b	Probabilistic Distribution Method
Gumbel	$1/(1+n)$	Normal Distribution
Gringorten	$(r - 0.44)/(n + 0.12)$	Log-Normal Distribution
Cunnane	$(r - 0.4)/(n + 0.2)$	Log-Pearson Type III
Weibull	$r / (n+1)$	<i>“r is the rank of the rainfall, n is the total number of observations (years)”</i>

## 4.2. Probability Plotting Position Modules

### 4.2.1. Gumble plotting Position

Gumble plotting position was plotted in figure-4, then the residual and RMSE were estimated from this curve.

The return period “T” 3, 5, 10, 15, 25, 50, and 100 years and the return periods values “ $x_t$ ” results obtained from Gumble plotting position are summarized in table 6.

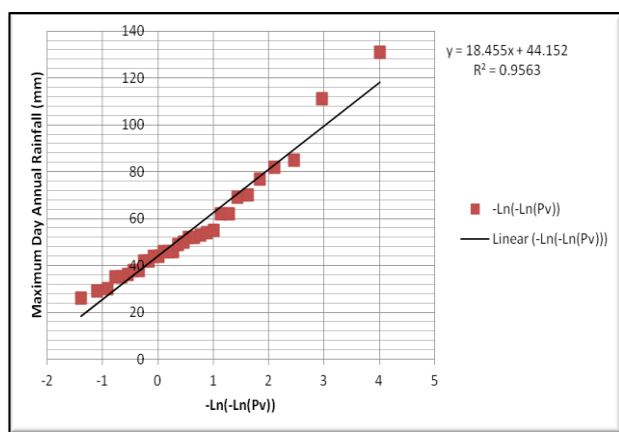


**Figure 4.** Gumble Plotting Position of rainfall distribution: The vertical axis represents the maximum rainfall (mm/day) and the horizontal axis is the quintiles of the percent point.

The maximum daily annual rainfall forms an approximately straight line depicting an excellent distribution to the model used [17]. The scale parameter is estimated by the slope of the trend line ( $\alpha = 18.4$ ) and the location parameter ( $\mu = 44.16$ ). The fitted function  $R^2 = 0.96$  indicates a proper adjustment of the distributed points. After extracting the location and the scale parameters of the Gumble distribution, the estimating of the extreme rainfall of the Area was possible.

### 4.2.2. Cunnane Plotting Position

Fitted function  $R^2 = 0.95$  for this plotting, shows a pretty adjustment of the distributed points. After determining the location ( $\mu = 44.11$ ) and scale parameters ( $\alpha = 18.61$ ) of the Cunnane plotting (Figure-5), estimating the extreme rainfall by using this plot, it was possible.

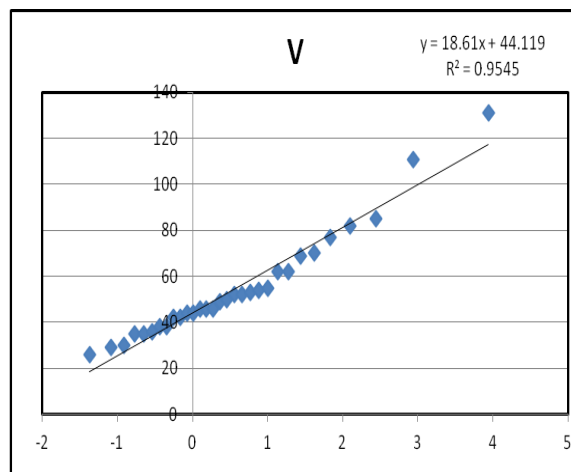


**Figure 5.** The Cunnane Plotting Position extreme value distribution of rainfall.

### 4.2.3. Weibull Plotting Position

The maximum daily rainfall (points on the graph) form a nearly straight line depicting a valid distribution to the model used. The scale parameter is estimated ( $\alpha = 19.93$ ) and the location parameter ( $\mu = 43.8$ ). The fitted function  $R^2 = 0.94$  shows a proper adjustment of the distributed points. After that, the extreme rainfall was estimated at the area by using Weibull plotting Position (Figure-6).

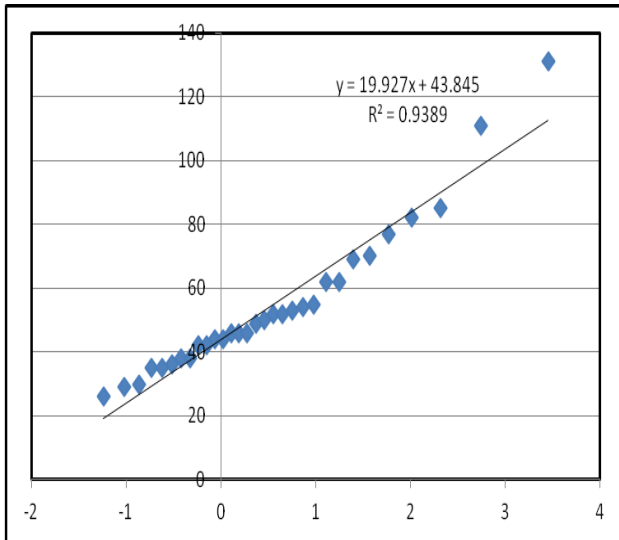


**Figure 6.** The Weibull Plotting Position extreme value distribution of rainfall.

**4.2.4. Gringorten Plotting Position**

The annual maximum rainfall forms a nearly straight line depicting a perfect distribution to the model used where the proper function ( $R^2= 0.96$ ) is shown in figure 7. The scale parameter is estimated ( $\alpha =18.33$ ) and the location parameter ( $\mu= 44.768$ ). By using these parameters, the extreme rainfall was expected of the area.

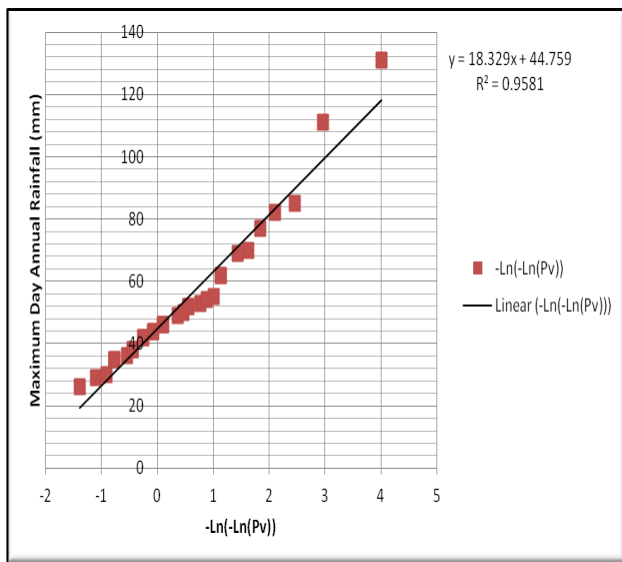


**Figure 7.** The Gringorten Plotting Position extreme value distribution of rainfall.

**4.3. Goodness-of-fit Test**

The results of the RSME values are listed in table 3. The values of the RMSE show that the lowest value is 5.57 for Gumble Plotting Position.  $R^2$  is the best fit

with 95.8, which is the best value among all plotting positions. Therefore, the Gumle is the best plotting position curve for area.

**Table 3.** the values of the statistical parameters.

Description	Symbol	Value
Mean (Average)	$\mu, X_{Avr}$	54.6 mm
Standard Deviation	$\sigma$	23.3 mm
Co-efficient of Variation	$C_V$	0.43
Co-efficient of Skewed SSkewedSkewness	$C_S$	1.69
Kurtosis of Distribution	$Ku$	3.3

The results of the Q-Q plots among the four plotting position and normal-log distribution (figure-8), the plots among the four plotting position and normal distribution (figure-9) and the plot among the four plotting position and the log-Pearson type III distribution (figure-10) show that the best-fit graphs are the log-Pearson type III. The best fit was the graphs between log-Pearson type III and the Gumle plotting position.

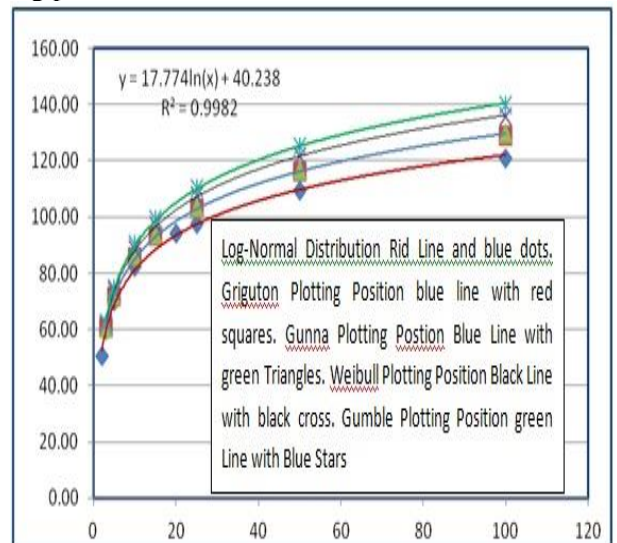


**Figure 8.** Log- Normal Distribution, with Griguton, Gunna, Weibull and Gumble plotting Positions.

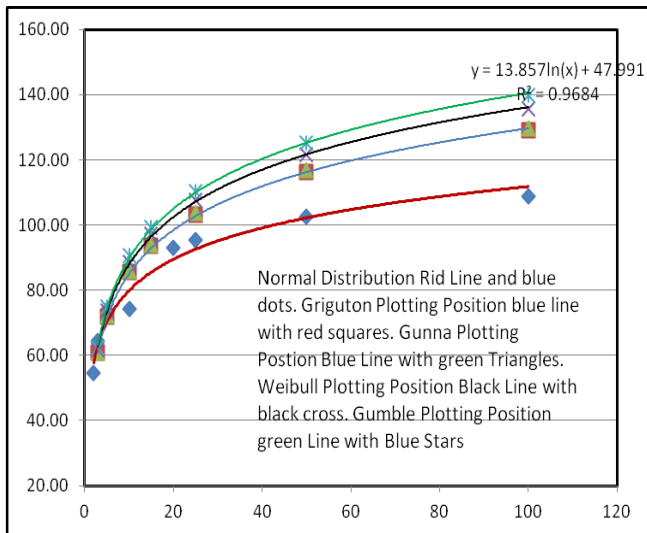


**Figure 9.** Normal Distribution, with Griguton, Gunna, Weibull and Gumble plotting Positions.

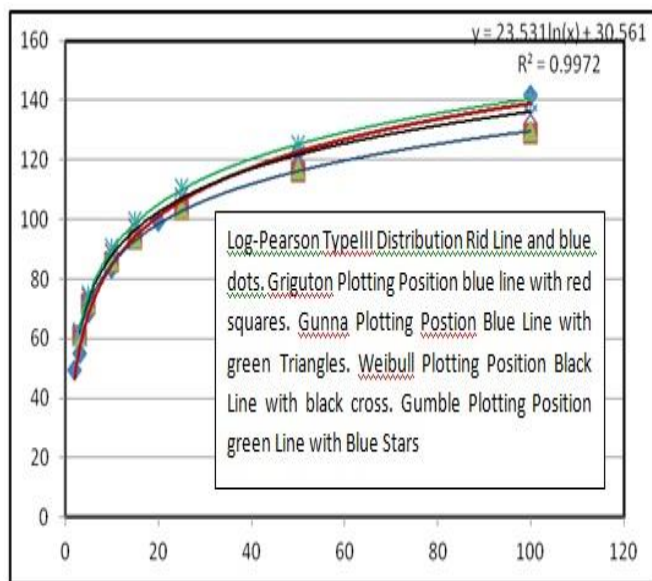


**Figure 10.** Log-Pearson Type III Distribution, with Griguton, Gunna, Weibull and Gumble plotting Positions.

**4.4. Return Periods “T” and Return Level “Xt”**

The results of the return periods (T) and return level (Xt) for the four plotting position graphs and the average of the four plotting positions are listed in table-4, and the results and the average of (T) and (Xt) for the three probability distributions are listed on table-5.

**Table 4.** the results of RSME for all the plotting positions.

Plotting Position	R2	RSME
Gumble	95.81	5.57
Gunnane	95.45	9.68
Weibull	93.9	6.01
Grington	95.6	6.1

**Table 5.** The results of return periods (T) and return level (Xt) for the four different plotting positions.

Plotting Positions	Return Periods (T) Years Return Level- Xt (mm)						
	3	5	10	20	25	50	100
Gumble	62.2	74.8	90.5	99.4	110.4	125.1	139.8
Gunna	60.9	72.0	86.0	93.9	103.6	116.7	129.7
Weibull	61.8	73.7	88.6	97.1	107.6	121.6	135.5
Grington	60.8	71.8	85.7	93.5	103.2	116.1	129.0
Average MAX. Daily rainfall	61.4	73.1	87.7	96	106	119.9	133.5

As a result, the return level (Xt) for the log-Pearson type III and the Gumble plotting position which has the lowest RMSE as the best fit values which are return periods of 3, 5, 10, 20, 25, 50, and 100 years have a return level (Xt) 62.2, 74.8, 90.5, 99.4, 110.4, 125.1 and 139.8 mm respectively as a maximum daily rainfall in the year. Due to high slope of the study area most of the rain and the surface water drains toward the Jordan Valley at the west of the study area. By estimating the catchment area of the Jordan Valley, we expect that the Jordan Valley will be flooded if the daily rain is more than 90 mm/day. Therefore, we expect that the Jordan Valley will be flooded in the year 2021 and so on every 10 years. Due to the lack of researches about the return periods for the study area that makes a comparison between my findings and previous results is too difficult.

**5. Conclusions**

This research has explained a probability modeling of maximum daily rainfall in Ajlun, Jordan, using different plotting positions and probability distributions. The maximum daily rainfall study for determining the best-fitted probability distributions revealed that the best probability distributions for the rainfall data set. The log-Pearson type-III and Gumbel were the best fit for the maximum daily rain of the study area. The maximum daily rainfall amounts relating to return periods of 3 to 100 years are

generated together with their uncertainties. Despite the good results of our analysis in this research, the estimations of the extreme return level values may have uncertain validity. Due to the lowering of the rainfall and the increase of the population in the study area, the area will suffer from water scarcity soon. On the other hand, we expect that the Jordan Valley will be flooded in the winter season in the year 2021 and so on every 10 years. Therefore the decision makers must take in their consideration of these results. They have to protect the farmers in the Jordan Valley from these flooding by building embankments and small dams along the Jordan Valley are on the drainage systems in the mountains surroundings the Jordan Valley.

## Acknowledgments

The author acknowledges Al-Balqa Applied University for its supporting in this research for offering a sabbatical leave.

## References

- [1] FAO. Coping with water scarcity - an action framework for agriculture and food security. FAO Water Report 38, Rome: Food and Agriculture Organization of the United Nations, 2012.
- [2] Krüger, O. and Graßl, H. The indirect aerosol effect over Europe. *Geophysical Research Letters* 29(19), 1925: doi:10.1029/2001GL014081, 2002.
- [3] Broska LH, Poganietz WR, Vogege S. Extreme events defined—a conceptual discussion applying a complex systems approach. *Futures* 115:102490, 2020
- [4] World Bank Report, Climate Change Adaptation and Natural Disasters Preparedness in the Coastal Cities of North Africa, World Bank, Washington, DC, pp. 34–35, <http://hdl.handle.net/10986/18708>, 2010
- [5] Hadadin, N.; Qaqish, M.; Akawwi, E; and Bdour, A. “Water shortage in Jordan - Sustainable solutions,” *Desalination*, vol. 250, no. 1, pp. 197–202, <https://doi.org/10.1016/j.desal.2009.01.026>, 2010.
- [6] Al-ansari, N.; Alibrahiem, N.; Alsaman, M.; and Knutsson, S. “Water Demand Management in Jordan,” *Engineering*, vol. 6, no. January, pp. 19–26, doi: [10.4236/eng.2014.61004](https://doi.org/10.4236/eng.2014.61004), 2014.
- [7] Abdulla, F.; Eshtawi, T.; Assaf, H. Assessment of the impact of potential climate change on the water balance of a semi-arid watershed. *Water Resour. Manag.* 23, 2051–2068, doi: [10.1007/s11269-008-9369-y](https://doi.org/10.1007/s11269-008-9369-y), 2009.
- [8] Parry, M., Arnell, N., McMichael, T., Nicholls, R., Martens, P., Kovats, S., Livermore, M., Rosenzweig, C., Iglesias, A., and Fischer, G. Millions at risk: defining critical climate change threats and targets. *Global Environmental Change* 11: 181-183, [http://dx.doi.org/10.1016/S0959-3780\(01\)00011-5](http://dx.doi.org/10.1016/S0959-3780(01)00011-5), 2001.
- [9] Arnell, N.W. ‘Climate change and global water resources: SRES emissions and socio-economic scenarios’, *Global Environmental Change* 14: 31-52, <https://doi.org/10.1016/j.gloenvcha.2003.10.006>, 2004
- [10] Upadhaya and Singh, Estimation of consecutive days maximum rainfall by various methods and their comparison, *Indian Journal of soil conservation* 26 (2), 193-200, 1998.
- [11] Omran, Z. A., Al-Bazzaz, S. T., & Ruddock, F. Statistical Analysis of Rainfall Records of Some Iraqi Meteorological Stations, *Journal of Babylon University/Engineering Sciences/ No. (1)/ Vol. (22):* 2014.
- [12] Ashraful Alam, Kazuo Emura, Craig Farnham and Jihui Yuan, Best-Fit Probability Distributions and Return Periods for Maximum Monthly Rainfall in Bangladesh, *Climate*, 6(9), <https://doi.org/10.3390/cli6010009>, 2018.
- [13] Abdullah A. Abbas, Nashaat A. Ali, Gamal Abozeid, and Hassan I. Mohamed, COMPARISON OF DIFFERENT METHODS FOR ESTIMATING MISSING MONTHLY RAINFALL DATA, Twenty-Second International Water Technology Conference, IWTC22, Ismailia, 12-13 September 2019
- [14] Markovic, R.D. Probability Functions of Best Fit to Distributions of Annual Precipitation and Runoff; Colorado State University Hydrology Paper No. 8; Colorado State University: Fort Collins, CO, USA, 1965.
- [15] Vogel, R.M.; Kroll, C.N. Low-Flow Frequency Analysis Using Probability-Plot Correlation Coefficients. *J. Water Resour. Plan. Manag.*, 115, 338–357, [https://doi.org/10.1061/\(ASCE\)0733-9496\(1989\)115:3\(338\)](https://doi.org/10.1061/(ASCE)0733-9496(1989)115:3(338)), 1989.
- [16] Cunnane, C. Unbiased plotting positions—A review. *J. Hydrol.* 37, 205–222, [https://doi.org/10.1016/0022-1694\(78\)90017-3](https://doi.org/10.1016/0022-1694(78)90017-3), 1978.
- [17] Wilks, D.S. Comparison of three-parameter probability distributions for representing annual extreme and partial duration precipitation series. *Water Resour. Res.*, 29, 3543–3549, <https://doi.org/10.1029/93WR01710>, 1993.
- [18] Chamber, J.; Cleveland, W.; Kleiner, B.; Tukey, P. *Graphical Methods for Data Analysis*. Biometric, January 1983.

## Creative Commons Attribution License 4.0 (Attribution 4.0 International, CC BY 4.0)

This article is published under the terms of the Creative Commons Attribution License 4.0  
[https://creativecommons.org/licenses/by/4.0/deed.en\\_US](https://creativecommons.org/licenses/by/4.0/deed.en_US)



**Authors contributions:**

**The contribution of the first Author Emad was collect data, writing and editing the manuscript.**

**The contribution of the second Author Metri was read and editing the article.**

**Tables Capture**

**Table 1.** The Statistical Parameters that were used in this study.

**Table 2.** Plotting Position Methods and Probabilistic Distribution Methods.

**Table 3.** the values of the statistical parameters.

**Table 4.** the results of RSME for all the plotting positions.

**Table 5.** The results of return periods (T) and return level (Xt) for the four different plotting positions.

**Figures Capture**

**Figure 1.** Shows the map of drainage of the study area (the study area represents by rectangle in Jordan Map to the right).

**Figure 2.** the annual precipitation all over Jordan, Ajlun and Al-Salt governorates located within the range of 700 – 900 mm/Y.

**Figure 3.** Annual rainfall (Left) and the Maximum Day Annual Rainfall (Right) distributed for the period of 31 years (1988-2018).

**Figure 4.** Gumble Plotting Position of rainfall distribution: The vertical axis represents the maximum rainfall (mm/day) and the horizontal axis is the quintiles of the percent point.

**Figure 5.** The Cunnane Plotting Position extreme value distribution of rainfall.

**Figure 6.** The Weibull Plotting Position extreme value distribution of rainfall.

**Figure 7.** The Gringorten Plotting Position extreme value distribution of rainfall.

**Figure 8.** Log- Normal Distribution, with Griguton, Gunna, Weibull and Gumble plotting Positions.

**Figure 9.** Normal Distribution, with Griguton, Gunna, Weibull and Gumble plotting Positions.